

Effect of Button Geometry on TRIP800 Steel Resistance Spot Weldment

Hayriye Ertek Emre¹, Ramazan Kaçar²

Research Asistant, Department of Manufacturing Engineering, Karabük University, Karabük, Turkey¹

Professor, Department of Manufacturing Engineering, Karabük University, Karabük, Turkey²

ABSTRACT: TRIP steels which are used for automotive industry are usually welded by resistance spot welding. The welding current, welding time and electrode force are most important welding parameters which affect to properties of the resistance spot welded steels. In this study, the TRIP800 steels were joined with a constant electrode force and welding time by using various welding currents. An effect of welding current on the joint strength and weld button geometry; nugget diameter, nugget height and electrode indentation depth was investigated. It was found that the heat input related to the increasing welding current notably affects weld button geometry and mechanical properties. It was determined that the strength of the weldment increased up to critical button geometry later on it fall down. In addition, cross tensile test was also applied to the samples which were obtained by using optimum welding parameters. The fracture modes of test samples were evaluated and hardness measurements were also determined.

KEYWORDS: TRIP800 steels, Resistance spot welding, Welding current, Button geometry.

I. INTRODUCTION

Steel sheets used in the automotive industry are classified and identified according to their metallurgic design and strength [1-3]. According to classification by strength, the tensile strength of “Ultra-High Strength Steels” (UHSS) is above 700 MPa [4,5]. Car manufacturers have indicated that the TRIP steel (in UHSS steel groups) has the highest potential of reducing the weight of a car and absorbing sudden impacts within itself [6-8].

Among the welding methods used in the automotive industry, resistance spot welding has a significant position particularly in robotic applications. There are different studies conducted on resistance spot welding of TRIP steels [9-14]. In one of these studies, Khan et al. detected undissolved ferrite and martensite in the weld nugget of TRIP780 steels, as well as a small amount of untransformed retained austenite phases in the heat affected zone (HAZ) of such steels. They reported that in comparison to conventional steels, the strength of joints made with these steels is much higher and that failure occurs in the pullout mode [15]. The weldability of other steels with TRIP steels were compared by Shi and Westgate [16]. The researchers emphasized that a higher electrode pressure force was required to be applied during welding processes due to the fact that TRIP steels contain more carbon [16]. Kim et al., on the other hand, reported that welding of galvanized TRIP steels required a higher welding current and longer welding time due to having less weldability in comparison to ungalvanized steels [17]. It was also reported that the increase of hardness which occurred in the weld nugget of the TRIP700 steel was lowered while the brittleness in the area was reduced to a certain extent [18]. In another study, Long et al. carried out fatigue and damage analyses in resistance welded connections of the DP600, TRIP600 and HSLA340YGI steels used in automotive industry and it was stated that the cracks formed under both low and excessive loading conditions progressed vertically towards the joint interface [19].

A review of the literature on the subject revealed no detailed studies about the strength of TRIP steel weldments and the effect welding current has on the weld nugget geometry. Therefore, based on the welding current, nugget diameter, d_n , nugget cross section height, h_n , nugget diameter/nugget height ratio, d_n/h_n , electrode indentation, e_i of the weld geometry were determined. At the same time, tensile shear and cross tensile strengths of the joints were identified as well.

International Journal of Innovative Research in Science, Engineering and Technology

(An ISO 3297: 2007 Certified Organization)

Vol. 5, Special Issue 12, May 2016

II. EXPERIMENTAL PROCEDURE

TRIP800 steel sheets in 1.5 mm thickness were used for experimental processes. The chemical composition of steel is given in Table 1. A timer and current controlled resistance spot welding machine having 60 kVA capacity and pneumatic application mechanisms with a single lever was used in experiments. The electrode force was continuously measured and controlled at fixed 6 kN force during the experiments. The welding time, clamping and holding times were kept constant as 15 cycles in all series. The welding current was increased from 1 to 10 kA by increasing 1kA. Spherical tip electrodes (CuCrZr) having 5.5 mm sphere diameter were used in the experiments. The parameter used for joining of the spot weld samples is shown in Table 2. (1 cycle period means 0.02 second).

Table. 1 Chemical composition of TRIP 800 steel (% wt).

Material	C	Si	Mn	P	S	Cr	Mo	Al	Fe
TRIP800	0,2	1,66	1,69	0,015	0,0002	0,006	0,01	0,43	Bal.

Table. 2 Welding parameters.

Welding current (kA)	Electrode force (kN)	Welding time (cycle)	Hold time (cycle)	Squeeze time (cycle)	Clamping time(cycle)
1-10	6	15	15	25	15

Welded samples were exposed to tensile shear test for determining joint strength while the cross tensile tests were also applied for samples that generated maximum tensile shear strength. The tensile shear and cross tensile sample assemblies are shown in Fig. 1 (a) and (b). Five test samples were prepared and tested for each parameters by using Shimadzu testing machine at a cross head of 5 mm/min.

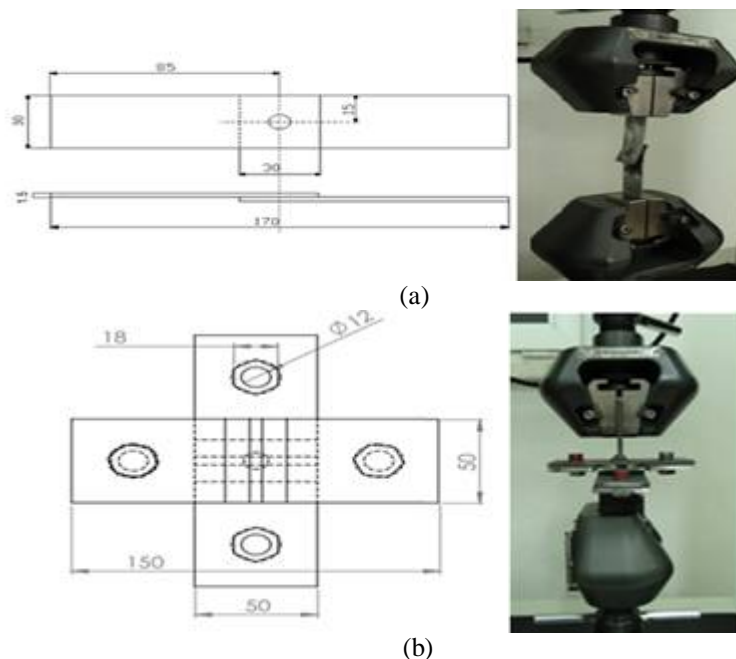


Fig. 1. Schematic specimen and testing representation of (a) tensile-shear, (b) cross-tensile specimen

International Journal of Innovative Research in Science, Engineering and Technology

(An ISO 3297: 2007 Certified Organization)

Vol. 5, Special Issue 12, May 2016

The failure modes were evaluated from the tested samples by using Zeiss Ultra Plus type SEM microscope. The weld nugget geometry; d_n , h_n , and e_i were measured on the cross section sample (Fig 2). In addition h_n/d_n ratio was calculated and its effect on the mechanical properties was determined. The samples were etched for 5 s with 2 % nital. Hardness measurements were carried out from base metal to the weld nugget by using a Shimadzu micro hardness tester by using 500 g load (Fig 2).

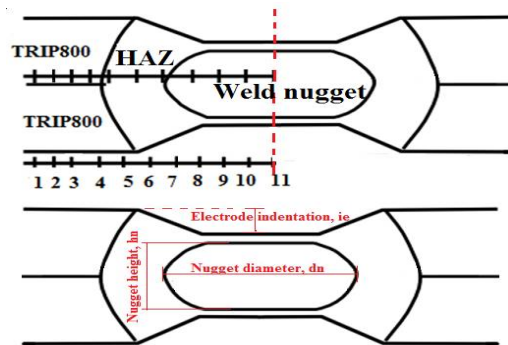


Fig. 2. Microhardness measurements and weld geometry profile.

III. RESULTS AND DISCUSSIONS

It is known that the strength of weldment is substantially affected by the nugget geometry, h_n , d_n and e_i which depend on welding parameters. [20,21]. The d_n and h_n changes are not the sole factors that influence strength. It is known that the heat input and electrode indentation increase which are affected by welding parameters influence the h_n/d_n ratio and thus, the strength [20]. Therefore, the h_n , d_n and e_i of the weldment were measured over the macrograph which was taken from the cross section of the weld joint and demonstrated in Figure 3.

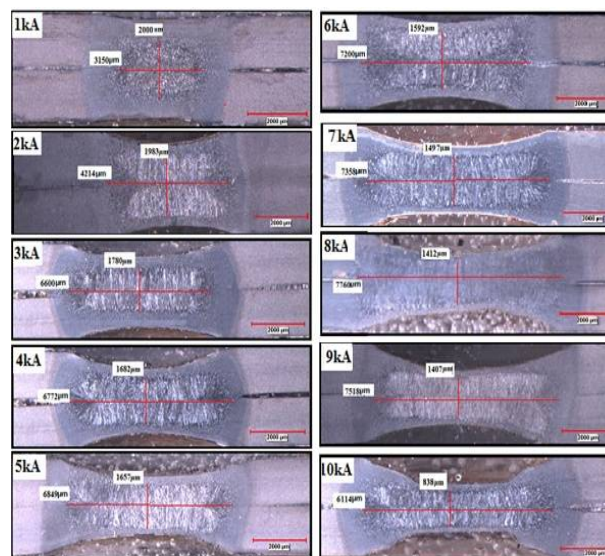


Fig. 3 The macrostructure of welded sample which joined with different welding current.

The welding current used in the experimental study and the tensile shear strength change of the weldments which depend on d_n , h_n , e_i , and h_n/d_n ratio changes are graphically shown in Figure 4 (a)-(d) respectively.

International Journal of Innovative Research in Science, Engineering and Technology

(An ISO 3297: 2007 Certified Organization)

Vol. 5, Special Issue 12, May 2016

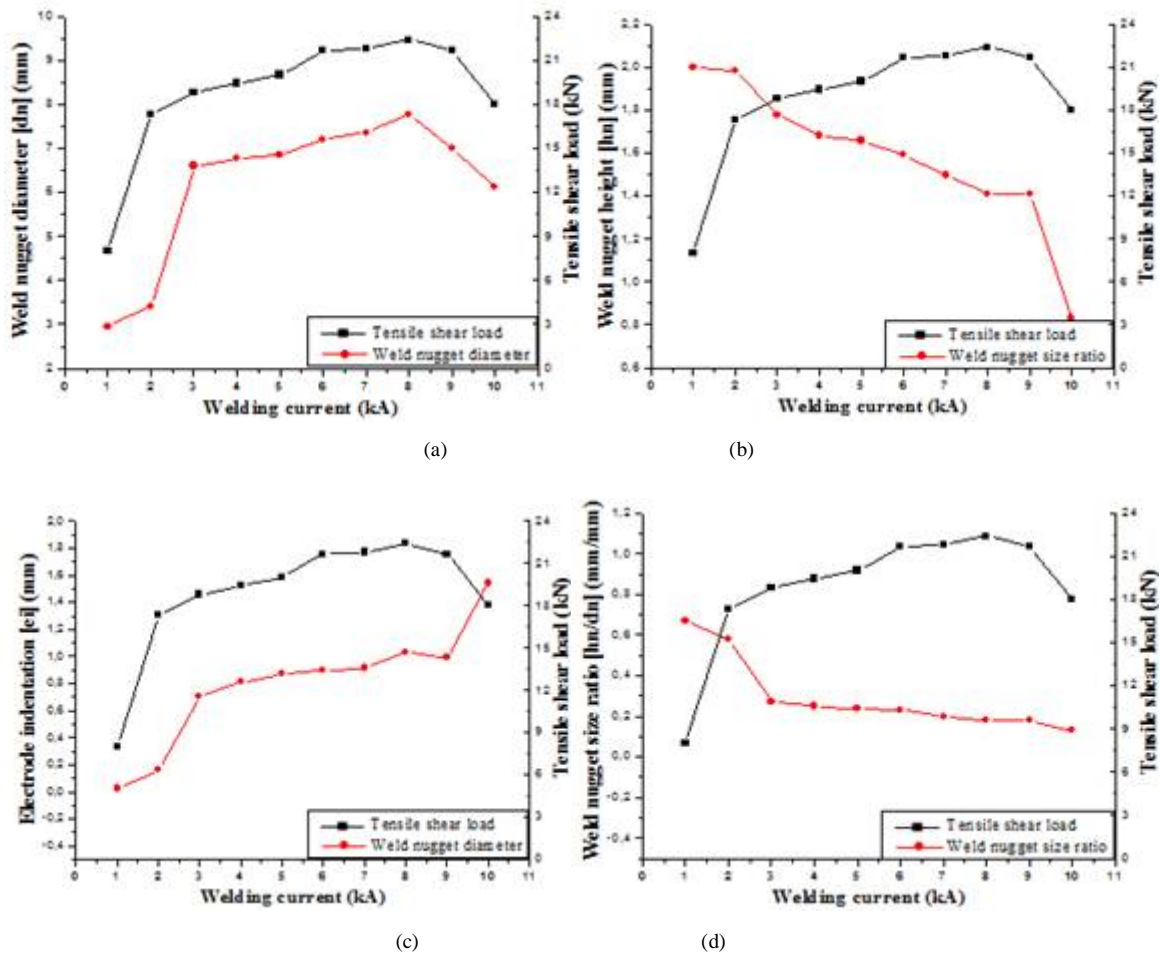


Fig. 4 The relationship of (a) weld nugget diameter, (b) weld nugget height, (c) electrode indentation, (d) nugget size ratio between welding current and tensile shear load.

As seen in Fig. 4 (a), a noticeable growth is seen in nugget diameter due to the heat input increase in parallel with welding current increases up to 8 kA; on the other hand, welding current higher than 8 kA caused the nugget diameter to shrink due to expulsion. Similarly, it was reported that the nugget diameter which grows as heat input increases contracts due to expulsion and spurting over a certain value [22-25]. The growth of the nugget size improved the strength of the joint (Fig. 4 (a)). Wan et al. and Kong et al. [26, 27] reported that increasing welding current positively affect the strength of joints. It was also reported that the heat input which increases in parallel with the rise in welding current extends the size of the fusion zone, which in turn enhances strength [28-30]. Vural and Akkuş [31] stated that an increase in the welding current up to a critical value leads to a rise in d_n , which causes the strength to increase at first; however they also stated that after the critical welding current value is exceeded, the d_n and the strength is decreased due to expulsion. In another study, it is reported that the nugget diameter grows and flattens as welding current and welding time increases, which in return causes the strength to rise; it is also reported that after a certain degree of flattening, penetration is reduced and the strength decreases [28-33].

International Journal of Innovative Research in Science, Engineering and Technology

(An ISO 3297: 2007 Certified Organization)

Vol. 5, Special Issue 12, May 2016

As can be seen in Figure 4 (b) and (c), the increasing welding current caused the e_i to rise and h_n to decrease noticeably. The strength decreased in parallel with a decline in h_n section. The fact that e_i increases while h_n decreases excessively in samples connected with welding current over 8 kA indicates that the heat input for TRIP800 steel is very high. As can be seen in Figure 4 (b), the nugget section thickness varied between 1.4 and 1.6 mm at the welding current range of 6-8 kA where optimum strength is acquired and a considerable decrease was detected in the nugget h_n value of samples connected with welding current over 8 kA as the e_i increased. Figure 4 (c) indicates that maximum strength was acquired within a welding current range of 6-8 kA and an e_i range of 0.9-1 mm, and shows that the desired d_n cannot be achieved under the aforementioned e_i value while going over this value once again leads to inability to achieve the desired strength due to excessive fusion and spurting. Figure 4 (d) demonstrates that as the h_n/d_n ratio decreases in parallel with welding current increases, the acceptable value of strength is obtained at the welding current range of 6-8 kA while the range of the h_n/d_n ratio is 0.15-0.22 and that the preferred amount of strength cannot be acquired under or over this range.

A cross tensile test was applied to weldments at parameters which the maximum tensile shearing strength value is achieved and the results are shown in Figure 5.

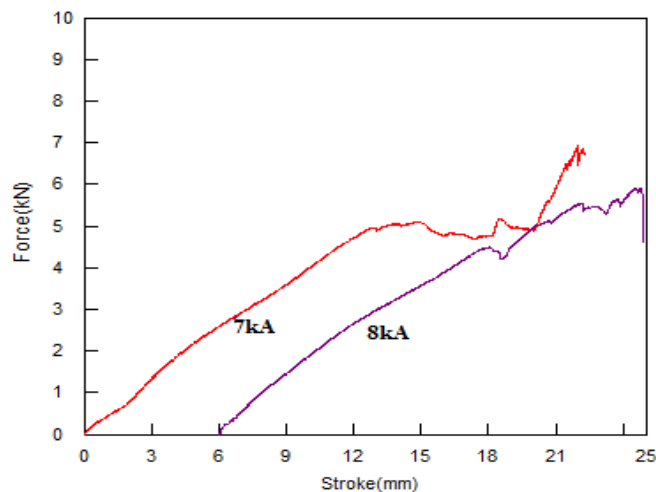


Fig. 5 Cross tensile test graphics.

As can be seen in Figure 5, the cross tensile strength values of samples joined with welding current of 7 and 8 kA were determined respectively as 5.1 kN and 5.9 kN. The increase in welding current led to a rise in the cross tensile strengths of weldments, in parallel with the tensile shear test. The test resulted in pullout failure mode in the HAZ. Pullout failure indicates that the weldment will have sufficient strength when forced to split with a static force. The correctness of the optimum welding parameters determined through the tensile shear test are thus confirmed by the cross tensile test. SEM images acquired from the fracture surfaces formed after the test are shown in Figure 6.

As seen in Figure 6, the fracture surface images display the type of cleavage fractures, associated with the hard phases in the structure of the resistance welded samples (Figure 6 a,c). A semi-dendritic and semi-brittle fracturing is indicated in the nugget HAZ interface in relation to structural transformation (Figure 6 b, d). It is believed that the crack began around the nugget during the test.

International Journal of Innovative Research in Science, Engineering and Technology

(An ISO 3297: 2007 Certified Organization)

Vol. 5, Special Issue 12, May 2016

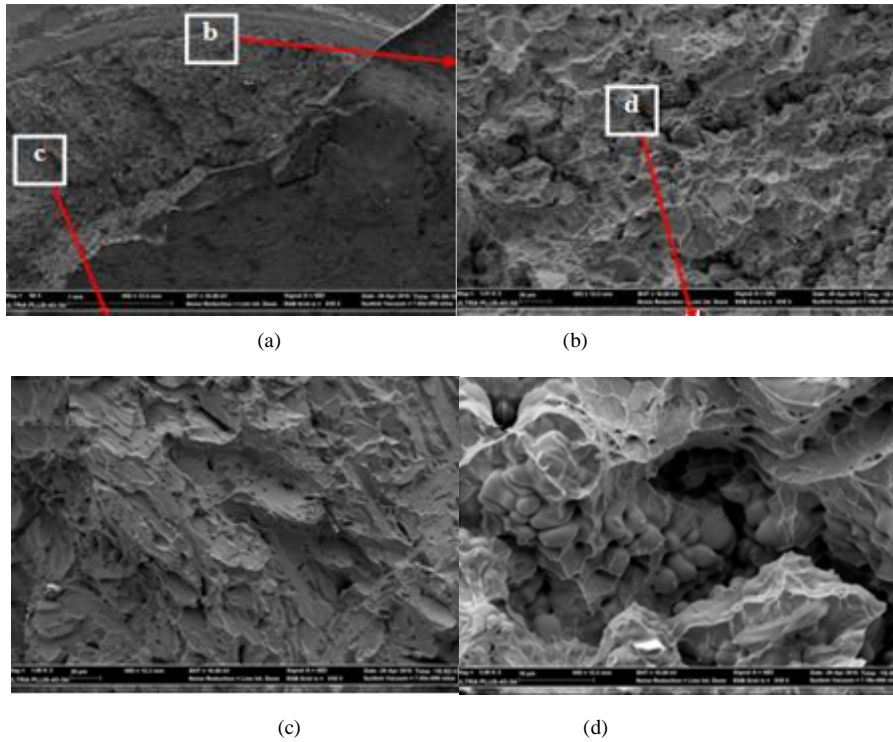


Fig. 6 Fracture surface acquired after the cross tensile test, (a) macro view, (b),(d) weld nugget-HAZ interface, (c) weld nugget.

The hardness distributions of the samples resistance spot welded with different welding current are graphically shown in Figure 7.

As can be seen in Figure 7, the hardness increases considerably in the HAZ and the weld nugget, compared to the base metal. While the base metal hardness value is 255 HV_{0.5}, nugget hardness value varies between 540 and 550 HV_{0.5}. The high hardness can be associated with the transformation into martensite phases due to rapid heating and cooling during the welding process.

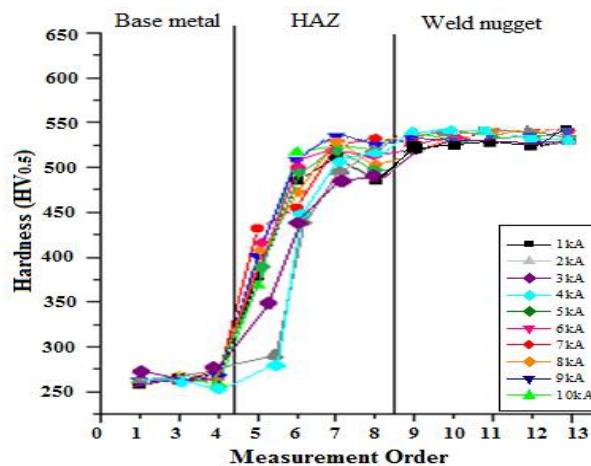


Fig. 7 Hardness profile of the weldment.

International Journal of Innovative Research in Science, Engineering and Technology

(An ISO 3297: 2007 Certified Organization)

Vol. 5, Special Issue 12, May 2016

It was detected that an increase in welding current, which can also be expressed as an increase in heat input, leads to a small change in the nugget and HAZ hardness, depending on the volume of the martensite phase formed in the structure. It is reported in similar studies that the hardness values of weld nugget vary between 400 and 550 HV_{0.5}, depending on the carbon content of TRIP steels [34-35].

IV. CONCLUSIONS

The findings acquired in the study are summarized below:

- The d_n and e_i increased as the welding current increased up to 8 kA, which led to a rise in tensile shear strengths of weldments. However the d_n and strength of weldments made with welding current over 8 kA decreased due to expulsion as the e_i continued to increase.
- As electrode indentation, e_i increased and h_n became thinner, the h_n/d_n ratio decreased. Since a smaller value of d_n was acquired due to insufficient heat input with lower welding current, the strength in weldments made with these was too low.
- The desired and accepted strength is acquired with a welding current of 6-8 kA, h_n of 1.4-1.6 mm, e_i of 0.9-1 mm and h_n/d_n ratio of 0.15-0.22. Since the desired d_n cannot be achieved below these ranges and expulsion occurs above these, the strength that is obtained is insufficient.
- The cross tensile strength resulted in pullout failure in the HAZ around the nugget. While the fracturing was brittle in the weld nugget, it was semi-dendritic and semi-brittle in the weld nugget HAZ interface, associated with the structural transformation.
- In comparison to the base metal, the hardness increased considerably in the HAZ and the weld nugget. The high value of hardness in the weld nugget can be associated with the transformation into martensite phases due to rapid heating and cooling during the welding process.

V. ACKNOWLEDGEMENT

This study was supported by Karabük University, Project Office. The authors would like to thank for their kind supports.

REFERENCES

- [1] S. Sharifimehr, A. Fatemi, S.C. Cha, M.K. Bae and S.H. Hong, "Fatigue behavior of AHSS lap shear and butt arc welds including the effect of periodic overloads and underloads", *International Journal of Fatigue*, vol.87, pp. 6–14, 2016.
- [2] M. Shome and M. Tumuluru, "Introduction to welding and joining of advanced high-strength steels (AHSS)", *Welding and Joining of Advanced High Strength Steels (AHSS)*, pp. 1-8, 2015.
- [3] A. Grajcar, R. Kuziak and W. Zalecki, "Third generation of AHSS with increased fraction of retained austenite for the automotive industry", *Archives of Civil and Mechanical Engineering*, vol. 12, no. 3, pp. 334–341, 2012.
- [4] M.I. Latypova, S. Shin, B.C.D. Cooman and H.S. Kim, "Micromechanical finite element analysis of strain partitioning in multiphase medium manganese TWIP+TRIP steel", *Acta Materialia*, vol. 108, pp. 219–228, 2016.
- [5] G. Azizi, H. Mirzadeh and M.H. Parsa, "The effect of primary thermo-mechanical treatment on TRIP steel microstructure and mechanical properties", *Materials Science and Engineering: A*, vol. 639, pp. 402–406, 2015.
- [6] H.K. Zeytin, G. Güven and B. Berme, "Conventional and modern sheet metals", *International Iron & Steel Symposium, Karabuk, Turkey*, pp. 434-447, 2012.
- [7] K. Ushioda, "Recent developments in steel sheets", *Scandinavian Journal of Metallurgy*, vol. 28, pp. 33-39, 1999.
- [8] W.J. Dan, S.H. Li, W.G. Zhang and Z.Q. Lin, "The effect of strain-induced martensitic transformation on mechanical properties of TRIP steel", *Materials and Design*, vol. 29, no. 4, pp. 604-612, 2008.
- [9] Z. Yinghui, M. Yonli, K. Yonglin and Y. Hao, "Mechanical properties and microstructure of TRIP steels produced using TSCR process", *Journal of University of Science and Technology, Beijing*, vol. 13, no. 5, pp. 416-421, 2006.
- [10] D. Wu, L. Zhuang and L. Hui-sheng, "Effect of controlled cooling after hot rolling on mechanical properties of hot rolled TRIP steel", *Journal of Iron and Steel Research International*, vol. 15, no. 2, pp. 65-70, 2008.
- [11] S. Koh-Ichi, M. Toshiki, H. Shun-Ichi and M. Yoichi, "Formability of Nb bearing ultra high strength TRIP-aided sheet steels", *Journal of Materials Processing Technology*, vol. 177, no. 1, pp. 390–395, 2006.
- [12] L. Skoalova, R. Divišová and D. Jandová, "Thermo-mechanical processing of low-alloy TRIP steel", *Journal of Materials Processing Technology*, vol. 175, no. 1, pp. 387–392, 2006.
- [13] S. Wen, L. Lin, B.C.D. Cooman, P. Wollants and C. Yang, "Thermal stability of retained austenite in TRIP steel after different treatments", *Journal of Iron and Steel Research International*, vol. 15, no. 1, pp. 61-64, 2008.

International Journal of Innovative Research in Science, Engineering and Technology

(An ISO 3297: 2007 Certified Organization)

Vol. 5, Special Issue 12, May 2016

- [14] L. Zhuang, W. Di and H. Rong, "Austempering of hot rolled Si-Mn TRIP steels", *Journal of Iron and Steel Research International*, vol. 13, no. 5, pp. 41-46, 2006.
- [15] M.I. Khan, M.L. Kuntz, E. Biro and Y. Zhou, "Microstructure and mechanical properties of resistance spot welded advanced high strength steels", *Materials Transactions*, vol. 49, no. 7, pp. 1629-1637, 2008.
- [16] G. Shi and S.A. Westgate, "Resistance spot welding of high strength steels", *Eleventh International Conference on the Joining of Materials*, Helsingor, Denmark, 2003.
- [17] T. Kim, H. Park and S. Rhee, "Optimization of welding parameters for resistance spot welding of TRIP steel with response surface methodology", *International Journal of Production*, vol. 43, no. 21, pp. 4643-4657, 2005.
- [18] G. Shi and S.A. Westgate, "Techniques for improving the weldability of trip steel using resistance spot welding", *1st International Conference Super-High Strength Steels*, Rome, Italy, 2005.
- [19] X. Long and S.K. Khanna, "Fatigue properties and failure characterization of spot welded high strength steel sheet", *International Journal of Fatigue*, vol. 29, pp. 879-886, 2007.
- [20] S. Aslanlar, "The effect of nucleus size on mechanical properties in electrical resistance spot welding of sheets used in automotive industry", *Materials & Design*, vol. 27, pp. 125-131, 2006.
- [21] X.Q. Zhang, G.L. Chen and Y.S. Zhang, "Characteristics of electrode wear in resistance spot welding dual-phase steels", *Materials & Design*, vol. 29, no. 1, pp. 279-283, 2008.
- [22] B. Kocabekir, R. Kaçar, S. Gündüz and F. Hayat, "An effect of heat input, weld atmosphere and weld cooling conditions on the resistance spot weldability of 316L austenitic stainless steel", *Journal of Materials Processing Technology*, vol. 195, pp. 327-335, 2008.
- [23] I. Sevim, F. Hayat and M.K. Kulekci, "Nucleus geometry and mechanical properties of resistance spot welded coated-uncoated DP automotive steels", *Bull. Mater. Sci.*, vol. 36, no. 6, pp. 1049-1055, 2013.
- [24] F. Hayat, B. Demir, M. Acarer and S. Aslanlar, "Effect of weld time and weld current on the mechanical properties of resistance spot welded IF (DIN EN 10130-1999) steel", *Kovove Materials*, vol. 47, no. 1, pp. 11-17, 2009.
- [25] I.S. Hwang, M.J. Kang and D.C. Kim, "Expulsion reduction in resistance spot welding by controlling of welding current waveform", *11th International Conference on the Mechanical Behavior of Materials*, vol. 10, pp. 2775-2781, 2011.
- [26] X. Wan, Y. Wang and P. Zhang, "Modelling the effect of welding current on resistance spot welding of DP600 steel", *Journal of Materials Processing Technology*, vol. 214, no. 11, pp. 2723-2729, 2014.
- [27] J.P. Kong, T.K. Han, K.G. Chin, B.G. Park and C.Y. Kang, "Effect of boron content and welding current on the mechanical properties of electrical resistance spot welds in complex-phase steels", *Materials & Design*, vol. 54, pp. 598-609, 2014.
- [28] P. Marashi, M. Pournavari, S. Amirabdollah, A. Abedi and M. Goodarzi, "Microstructure and failure behavior of dissimilar resistance spot welds between low carbon galvanized and austenitic stainless steels", *Materials Science and Engineering A*, vol. 480, pp. 175-180, 2008.
- [29] S. Fukumoto, K. Fujiwara, S. Toji and A. Yamamoto, "Small-Scale resistance spot welding of austenitic stainless steels", *Materials Science and Engineering A*, vol. 492, no. 1-2, pp. 243-249, 2008.
- [30] D. Özyürek, "An effect of weld current and weld atmosphere on the resistance spot weldability of 304L austenitic stainless steel", *Materials and Design*, vol. 29, pp. 597-603, 2008.
- [31] M. Vural and A. Akkuş, "On the resistance spot weldability of galvanized interstitial free steel sheets with austenitic stainless steel sheet", *Journal of Materials Processing Technology*, vol. 1, no. 6, pp. 153-154, 2004.
- [32] N. Ma and H. Murakawa, "Numerical and experimental study on nugget formation in resistance spot welding for three pieces of high strength steel sheets", *Journal of Materials Processing Technology*, vol. 210, no. 14, pp. 2045-2052, 2010.
- [33] M. Vural, A. Akkuş and B. Eryürek, "Effect of welding nugget diameter on the fatigue strength of the resistance spot welded joints of different steel sheets", *Journal of Materials Processing Technology*, vol. 176, no.1-3, pp. 127-132, 2006.
- [34] L. Cretteur, A.I. Koruk, L. Tosal-Martinez, "Improvement of weldability of TRIP steels by use of in-situ pre- and post-heat treatments", *Steel Res.*, vol. 73, pp. 314-319, 2002.
- [35] P. Burgmann, K. Clymer, S. Cobb, J. Davis, M. Liu, M. Miller, A. O'Loughlin, M. Smith, K.O. Findley and S. Liu, "Processing, microstructure and mechanical behavior relationships in advanced high-strength steel", *Iron Steel Technol.*, vol. 7, pp. 76-85, 2010.